Influences of Atlantic Climate Change on the Tropical Pacific via the Central American Isthmus*

SHANG-PING XIE

International Pacific Research Center, and Department of Meteorology, SOEST, University of Hawaii at Manoa, Honolulu, Hawaii

YUKO OKUMURA

National Center for Atmospheric Research, and UCAR Visiting Scientist, Boulder, Colorado

TORU MIYAMA

Frontier Research Center for Global Change, Yokohama, Japan

AXEL TIMMERMANN

International Pacific Research Center, and Department of Oceanography, SOEST, University of Hawaii at Manoa, Honolulu, Hawaii

(Manuscript received 11 September 2007, in final form 7 December 2007)

ABSTRACT

Recent global coupled model experiments suggest that the atmospheric bridge across Central America is a key conduit for Atlantic climate change to affect the tropical Pacific. A high-resolution regional ocean–atmosphere model (ROAM) of the eastern tropical Pacific is used to investigate key processes of this conduit by examining the response to a sea surface temperature (SST) cooling over the North Atlantic. The Atlantic cooling increases sea level pressure, driving northeasterly wind anomalies across the Isthmus of Panama year-round. While the atmospheric response is most pronounced during boreal summer/fall when the tropical North Atlantic is warm and conducive to deep convection, the Pacific SST response is strongest in winter/spring when the climatological northeast trade winds prevail across the isthmus. During winter, the northeasterly cross-isthmus winds intensify in response to the Atlantic cooling, reducing the SST in the Gulf of Panama by cold and dry advection from the Atlantic and by enhancing surface turbulent heat flux and mixing. This Gulf of Panama cooling reaches the equator and is amplified by the Bjerknes feedback during boreal spring. The equatorial anomalies of SST and zonal winds dissipate quickly in early summer as the seasonal development of the cold tongue increases the stratification of the atmospheric boundary layer and shields the surface from the Atlantic influence that propagates into the Pacific as tropospheric Rossby waves. The climatological winds over the far eastern Pacific warm pool turn southwesterly in summer/fall, superimposed on which the anomalous northesterlies induce a weak SST warming there.

The ROAM results are compared with global model water-hosing runs to shed light on intermodel consistency and differences in response to the shutdown of the Atlantic meridional overturning circulation. Implications for interpreting paleoclimate changes such as Heinrich events are discussed. The results presented here also aid in understanding phenomena in the present climate such as the Central American midsummer drought and Atlantic multidecadal oscillation.

1. Introduction

Heinrich events are characterized by ice-rafted detritus left on the seafloors of the high-latitude North Atlantic by massive glacial iceberg discharges from the Laurentide and possibly Eurasian ice sheets. Massive meltwater discharges into the North Atlantic during such Heinrich events and the more recent [~11 kyr before present (BP)] Younger Dryas event are believed

* International Pacific Research Center Publication Number 503 and School of Ocean and Earth Science and Technology Publication Number 7253.

Corresponding author address: Shang-Ping Xie, International Pacific Research Center, SOEST, University of Hawaii at Manoa, Honolulu, HI 96822.
E-mail: xie@hawaii.edu

DOI: 10.1175/2008JCLI2231.1

to have had a profound effect on the Atlantic meridional overturning circulation (AMOC) and the oceanic poleward heat transport. The associated climate effects in the North Atlantic region are well captured in annually resolving ice core records from Greenland. Recent marine sediment cores show that the influence of Heinrich events and the Younger Dryas is global, and not limited to the North Atlantic (Hemming 2004). Sea surface temperature (SST) and salinity at various tropical sites (Stott et al. 2002; Kienast et al. 2006; Pahnke et al. 2007) exhibit covariability with these abrupt climate perturbations that originated in the high-latitude North Atlantic region. It has been found that a North Atlantic cooling of about 10°C translates into a significant southward displacement of the Atlantic ITCZ, reducing rainfall over South America and the tropical Atlantic north of the equator (Peterson et al. 2000; Haug et al. 2001; Schmidt et al. 2006). On the Pacific side of the Central American isthmus, several recent analyses of sediment cores show that associated with high-latitude North Atlantic cooling, SST decreases and surface salinity increases in the northeastern tropical Pacific warm pool (Kienast et al. 2006; Leduc et al. 2007). However, the spatiotemporal fingerprints of Heinrich events or the Younger Dryas are complex with some parts of the eastern Pacific even becoming wetter (Pahnke et al. 2007) during North Atlantic millennial-scale cold periods.

Coupled ocean–atmosphere general circulation models (GCMs) support the notion that Heinrich events in the North Atlantic are capable of inducing major climatic anomalies around the globe, in partial accordance with recent paleoproxy evidence (Dahl et al. 2005; Menviel et al. 2008). So-called water-hosing experiments, in which freshwater is added to the North Atlantic (Manabe and Stouffer 1995), show that the resultant decrease in sea surface salinity and density leads to a slow down of the sinking branch of the AMOC with widespread repercussions for global climate. Recent coordinated efforts to conduct and compare water-hosing experiments with several state-of-the-art coupled ocean–atmosphere GCMs reveal a surprising degree of similarity among different models in terms of the global response pattern to a substantial weakening of the AMOC (Stouffer et al. 2006; Timmermann et al. 2007). A freshwater input of 1 Sv (10^6 $m^3\,s^{-1}$) to the subpolar North Atlantic, a magnitude probably achieved during typical Heinrich events, triggers a shutdown of the AMOC within a few decades in all of the models, inducing a major cooling in surface air temperature of up to 10°C over the subpolar North Atlantic and northern Europe.

This extratropical North Atlantic cooling intensifies the northeast trade winds, increasing surface evaporation and cooling the tropical Atlantic north of the equator. South of the equator, the southeast trades weaken and SST increases (Vellinga and Wood 2002), consistent with the wind–evaporation–SST (WES) feedback that preferentially amplifies ocean–atmospheric anomalies antisymmetrically about the equator (Xie and Philander 1994; Chang et al. 1997). The SST and wind anomalies over the Atlantic basin are remarkably consistent among the models (Timmermann et al. 2007), bearing some resemblance to a pan-Atlantic pattern observed on decadal time scales in instrumental observations that feature bands of SST anomalies of alternate signs stacked meridionally from the South Atlantic to Greenland (Xie and Tanimoto 1998; Tanimoto and Xie 2002; Chiang 2004). Such a pan-Atlantic pattern emerges in response to ice sheet forcing during the last glacial maximum in an atmospheric GCM coupled with a slab ocean model (Chiang et al. 2003), where the increased northeast trades trigger the WES feedback to form a meridional dipole in the tropical Atlantic. Using a partial coupling technique, Wu et al. (2008) and Krebs and Timmermann (2007) show, however, that the weakened AMOC and the resultant ocean dynamical adjustments are important for the tropical South Atlantic warming. There is some evidence that ocean circulation plays a role in the subtropical North Atlantic cooling in GCMs (Y. Okumura 2006, personal communication; Chiang et al. 2008).

In water-hosing experiments, the SST cooling north and warming south of the equator displace the Atlantic intertropical convergence zone (ITCZ) southward, much as observed in tropical Atlantic variability in modern climate [see Xie and Carton (2004) and Chang et al. (2006) for recent reviews]. Such a southward displacement of the Atlantic ITCZ is consistent with accumulating evidence based on a variety of paleoclimate reconstructions during Heinrich events and the Younger Dryas [Peterson et al. (2000); Haug et al. (2001); Schmidt et al. (2006), see Dahl et al. (2005) and Menviel et al. (2008) for a review].

Timmermann et al. (2007) identify the anomalous northeasterly winds across Central America as another robust feature in water-hosing experiments across models, in response to the SST cooling and increased atmospheric pressure over the tropical North Atlantic and in particular the Caribbean. All of the model simulations reproduce a cooling over the eastern Pacific warm pool north of the equator, consistent with recent analyses of sediment records (Kienast et al. 2006; Pahnke et al. 2007). However, the response is less consistent in the equatorial Pacific than in the tropical Atlantic. Some models favor a meridional dipole pattern similar to that

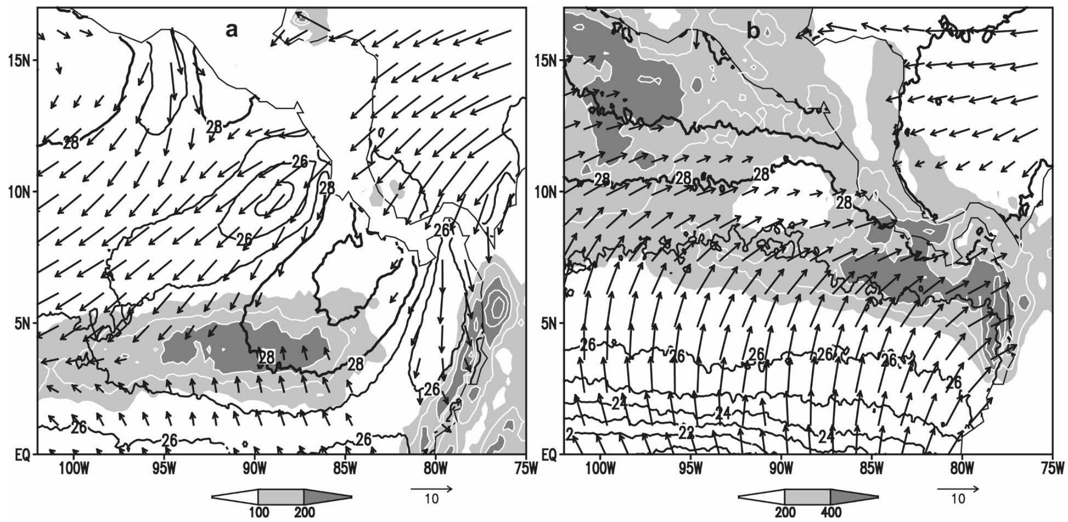

FIG. 1. Climatology of surface wind velocity (m s^{-1}), SST (black contours, °C), and precipitation (gray shade and white contours, mm month^{-1}) for (a) February and (b) September, based on Quick Scatterometer (QuikSCAT), Advanced Very High Resolution Radiometer (AVHRR), and Tropical Rain Measuring Mission (TRMM) satellite observations, respectively.

in the tropical Atlantic, with a southward-displaced ITCZ (Vellinga and Wood 2002; Zhang and Delworth 2005) while some others develop an El Niño– or La Niña–like pattern (Dong and Sutton 2002; Wu et al. 2007). What causes the differences in the simulated Pacific response to an AMOC weakening remains unclear. In those models with the anomalous southward displacement of the Pacific ITCZ, the reduced meridional asymmetry weakens the annual cycle on the equator, leading to an increase in the variance of the El Niño–Southern Oscillation (ENSO) because of the nonlinear frequency entrainment (Timmermann et al. 2007).

As manifested in northeasterly cross-isthmus wind anomalies in water-hosing experiments, atmospheric teleconnection across the Central American isthmus is an important conduit for Atlantic climate change to influence the tropical Pacific. By disabling the air–sea coupling over the tropical Atlantic in a water-hosing experiment, Wu et al. (2008) report that anomalies, including those of cross-isthmus winds, diminish over the eastern tropical Pacific. The Andes in South America and the Sierra Madre/Rockies in North America weaken the Atlantic influence on the lower atmosphere of the Pacific. Mountains over Central America play a major role in shaping the regional climate over the eastern Pacific warm pool. In the boreal winter climatology, the northeast trades blow across the isthmus, and three distinct wind jets form off the major gaps of the mountain range, in the Gulfs of Tehuantepec, Papagayo, and Panama (Chelton et al. 2000; Xie et al. 2005) (Fig. 1a). In addition, the orographic subsidence displaces the Pacific ITCZ southward from the eastern Pacific warm pool (Xu et al. 2005). Despite its climatic importance, the Central American isthmus is poorly represented in coupled GCMs used for water-hosing experiments. Typically, these models have horizontal resolutions of 200–300 km or coarser. The Central American isthmus is about a few hundred kilometers wide—the width at Panama is only about 100 km—and the mountain ranges on the isthmus are even narrower.

The present study investigates the Atlantic influences on tropical Pacific climate using a relatively high-resolution model that represents Central America and its mountains much better than do state-of-the art GCMs. The model consists of a full-physics regional atmosphere model spanning one-third of the tropical belt coupled with a Pacific basin ocean GCM. It simulates tropical Pacific climate and its seasonal cycle quite realistically (Xie et al. 2007). We impose a time-constant cooling over the North Atlantic and study the Pacific response. As it turns out, the Pacific response displays a pronounced seasonal dependence due to the strong seasonal cycle of the winds and the thermocline depth in the mean climate. For example, orographic effects of Central American mountains organize the northeast trades into well-defined gap wind jets in winter but surface winds converge onto Central America in summer, with the southwesterlies prevailing on the Pacific side (Fig. 1). Thus, the northeasterly wind anomalies strengthen the prevailing trades in winter but weaken the southwesterlies in summer, inducing opposite changes in the latent heat flux over the eastern Pacific warm pool. (Hereafter, seasons are for the Northern Hemisphere.) By focusing on the origin of the seasonality of Pacific anomalies, we aim to identify ocean–atmospheric processes and examine the mechanisms by which North Atlantic climate anomalies affect the Pacific through Central America. While motivated by water-hosing experiments and abrupt Atlantic climate changes, this study is also relevant to understanding the global impacts of the Atlantic multidecadal oscillation (AMO), a mode of climate variability possibly induced by AMOC variability (Delworth and Mann 2000; Timmermann et al. 1998).

The rest of the paper is organized as follows. Section 2 describes the model and experimental design. Section 3 examines the Pacific response and its seasonal dependence. Section 4 is a summary and discusses the implications for paleo- and present-day climate variability.

2. Model

We use a regional ocean–atmosphere model (ROAM) developed at the International Pacific Research Center (IPRC), University of Hawaii, in collaboration with the Frontier Research Center for Global Change (FRCGC), Japan. The horizontal resolution is 0.5° for both the ocean and atmospheric components. The atmospheric component is a full-physics regional model as in Wang et al. (2004), which has 28σ levels and covers one-third of the global tropics including the eastern Pacific and the entire tropical American continents (35°S–35°N, 150°–30°W). The model physics include a mass flux parameterization for convection, cloud microphysics, a radiation package interactive with clouds, a land surface model, and a nonlocal closure scheme for vertical turbulent mixing. The ocean component is the Modular Ocean Model version 2 developed at the Geophysical Fluid Dynamics Laboratory (Pacanowski 1996). It has 30 vertical levels and covers the entire tropical Pacific basin within 35°S–35°N. On the open boundaries, the atmospheric model is restored toward the 4-times-daily reanalysis of the National Centers for Environmental Prediction (NCEP) and National Center for Atmospheric Research (NCAR; Kalnay et al. 1996) while the ocean is restored toward the monthly Levitus (1982) climatology. The ocean and atmosphere are fully interactive in the eastern tropical Pacific east of 150°W. In the rest of the tropical Pacific to the west, the NCEP–NCAR atmospheric reanalysis is used to force the ocean model. In the tropical Atlantic, the observed weekly SST is prescribed.

The control simulation for 1996–2003, following a spinup of the ocean model, reproduces the salient features of the eastern Pacific climate, including a northward-displaced ITCZ, a stratus cloud deck south of the equator, the equatorial cold tongue, and their seasonal cycle (Xie et al. 2007). Internal air–sea feedbacks, such as that between SST and stratus cloud, are crucial to maintaining a realistic climatology (de Szoeke et al. 2006). See Xie et al. (2007) for a detailed description of the IPRC ROAM (iROAM) and its performance. De Szoeke and Xie (2008) compare the present-day simulations by the iROAM with 14 state-of-the-art coupled GCMs. The iROAM captures the major El Niño of 1997–98 (Fig. 2 of Xie et al. 2007), due mostly to the observed wind forcing prescribed in the western half of the Pacific basin.

a. Model climatology

Here, we focus on the far eastern Pacific off the Central American isthmus, the pathway for atmospheric teleconnections from the tropical Atlantic. Figure 2 shows the iROAM climatology of surface wind velocity and 20°C isotherm depth (Z20). During winter, the northeast trades intrude across Central America into the Pacific, meeting the southeast trades along 5°N at the ITCZ. The simulated northeast trades are organized into three wind jets downstream of the major mountain gaps of Tehuantepec, Papagayo, and Panama, much as in the observations. The simulated Panama jet is too weak and does not penetrate as far south as in the observations (Rodriquez-Rubio et al. 2003; Xie et al. 2005) (Fig. 1a), presumably because the insufficient model resolution underrepresents the orographic effects of the narrow mountains over Costa Rica. With increased (0.25°) resolution, the simulated Panama jet improves but still does not extend far enough south (Xu et al. 2005). In summer the ITCZ migrates northward following the seasonal march of the sun (Mitchell and Wallace 1992). In the far eastern tropical Pacific, the southerlies from the Southern Hemisphere gain a westerly component under the Coriolis force and converge onto Central America. Over the tropical North Atlantic, the northeast trades persist and converge onto the isthmus.

Orographic-induced wind jets imprint themselves strongly on the thermocline depth in winter. The thermocline shoals under the cyclonic curls of the wind jets. In particular, a thermocline dome forms south of the Papagayo jet, with Z20 attaining values of less than 30 m in the observations and simulation. This Costa Rica dome persists throughout the year, maintained in summer by the positive wind curls in the ITCZ. A thermocline trough forms along 4°–5°N just north of the shoaling equatorial thermocline. In winter this 5°N trough shallows by 20 m or more in response to the

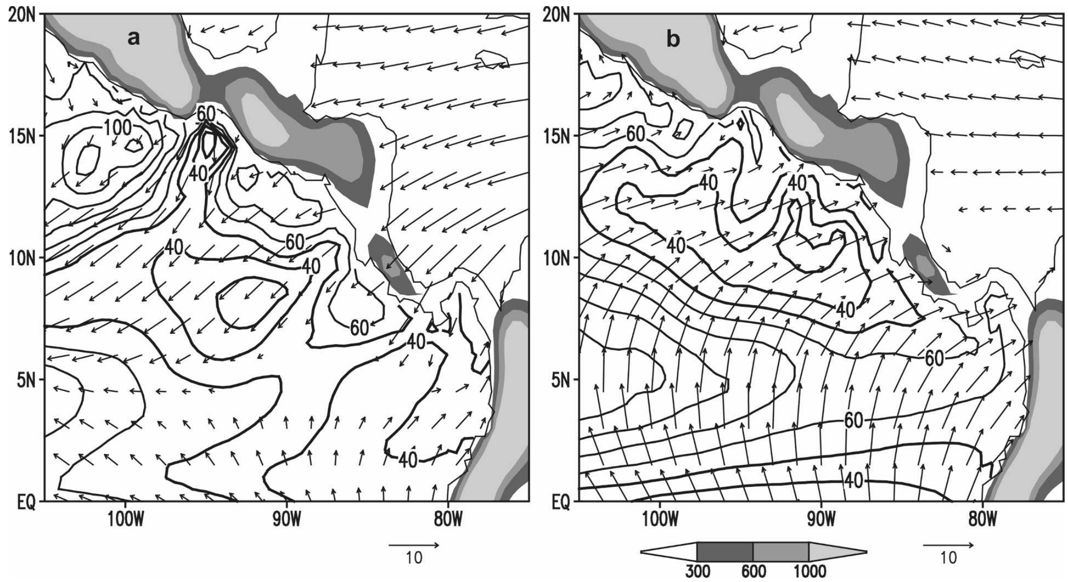

FIG. 2. Climatology of surface wind velocity (m s^{-1}) and the 20°C isotherm depth (m) in iROAM for (a) February and (b) August, along with land orography (gray shade, in m).

cyclonic curls of the overlying ITCZ. As will be demonstrated below, the winter shoaling of the thermocline is conducive to the equatorward propagation of the Atlantic influence into the eastern Pacific.

b. *Experimental design*

To investigate how Atlantic climate change affects the Pacific, we decrease the Atlantic SST by 2°C north of 5°N and taper this change off from 5°N to 5°S. The magnitude of the cooling over the tropical North Atlantic is typical of the changes simulated in GCM water-hosing experiments (Stouffer et al. 2006; Timmermann et al. 2007; Wu et al. 2008). In water-hosing runs of global GCMs, the North Atlantic cooling weakens in the subtropics and its tropical maximum displays little seasonal variations (Fig. 3 of Wu et al. 2008). Strictly speaking, our North Atlantic cooling experiment using the regional coupled model is not the same as the water-hosing experiments with global GCMs. In the latter, there are considerable anomalies over the Northern Hemisphere subtropics in both the atmosphere and oceans. [The North Pacific cooling weakens considerably with a closed Bering Strait as during the ice ages (Hu et al. 2008).] An alternative approach is to use the GCM output as lateral boundary conditions for the regional model, which will inevitably affect the model climatology. Here, we narrow the scope to investigate how the tropical Pacific responds to the North Atlantic cooling, disregarding the effects of atmospheric circulation changes near the boundaries of our modeling domain. Wu et al. (2008) and Krebs and Timmermann (2007, their Fig. 5d) show that SST anomalies over the tropical Atlantic are the most important contributor to the Pacific response in water-hosing experiments. The lateral boundary effects on the regional model simulation are left as a subject for future studies. The North Atlantic cooling (NAC) run covers the same 8-yr period from 1996 to 2003 as the control (CTRL). Our analysis focuses on the last 6 yr of these two experiments. In the NAC run, ocean–atmospheric anomalies develop quickly within the first 1–2 yr and reach a quasi-steady state thereafter. There is some moderate interannual variability in the coupled response in the NAC run but similar anomalies develop every year as represented by 6-yr averages to be discussed.

We carry out another set of experiments using the regional atmospheric model (RAM). In the RAM control run (CTRLa), the observed monthly SST is prescribed and the Pacific Ocean is decoupled with the atmosphere. In the RAM North Atlantic cooling (NACa) run, North Atlantic SST is lowered by 2°C as in the NAC run. The NACa minus CTRLa difference gives the atmospheric teleconnective forcing by the Atlantic cooling without air–sea interactions in the Pacific, while the (CTRL-NAC) minus (CTRLa − NACa) difference enables us to evaluate the coupled Pacific response to this atmospheric forcing.

3. Pacific response

Figure 3 shows the seasonal evolution of the SST and surface wind anomalies along the equator in response

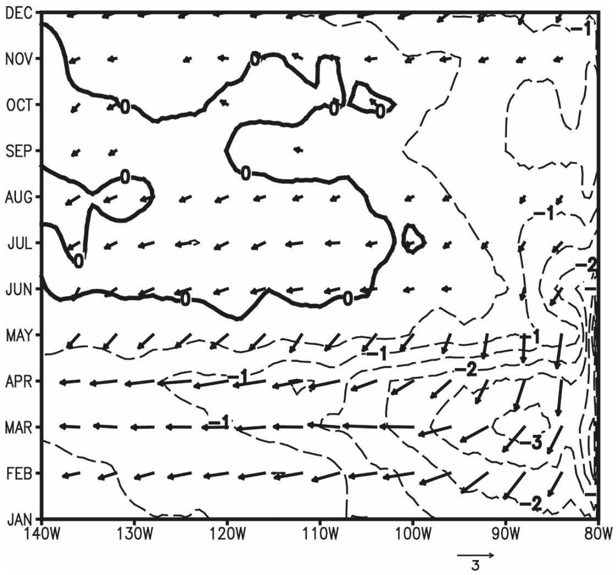

FIG. 3. Longitude–time cross section of SST (°C) and surface wind velocity (m s^{-1}) anomalies along the equator in the Atlantic cooling run of iROAM.

to the North Atlantic cooling, as computed from NAC − CTRL. An anomalous cold tongue develops during January–April that is associated with anomalous easterly winds, suggestive of the Bjerknes feedback. The equatorial anomalies decay rapidly in May and remain small until December. Climatological SST in the eastern equatorial Pacific displays a pronounced annual cycle, reaching its maximum in March and minimum in September. The strong cooling of up to −3°C in the NAC run during January–April represents a reduction in this annual cycle along the equator. This section examines the strong seasonality of the coupled response to the North Atlantic cooling.

a. *Boreal winter/spring*

Figure 4 tracks how the Atlantic cooling leads to the March–April cooling in the equatorial Pacific. In December, the equatorial Pacific SST anomalies are relatively small, generally less than 1°C. The imposed SST cooling over the tropical North Atlantic increases the atmospheric pressure by cooling the atmospheric boundary layer and reducing convection over tropical South America. The increased pressure over the North Atlantic drives an anomalous northeasterly wind jet of up to 5 m s^{-1} across the Isthmus of Panama, doubling the speed of the climatological jet. The intensified Panama jet cools the SST on its path. The cooling strengthens and reaches the equator in January. On the equator, the SST cooling in the east induces easterly wind anomalies, which reinforce the oceanic cooling by strengthening the upwelling and shoaling the thermocline by 20 m in the east (Fig. 5c). Thus, the Bjerknes feedback explains the equatorial amplification of SST anomalies once they reach the equator.

The anomalous wind jet and the SST cooling in the Gulf of Panama appear to trigger the Bjerknes feedback along the equator. To determine the processes leading to the Gulf of Panama cooling, we compare surface heat flux anomalies in response to Atlantic cooling in the forced atmospheric and the coupled model experiments (Fig. 5). In the RAM, the anoma-

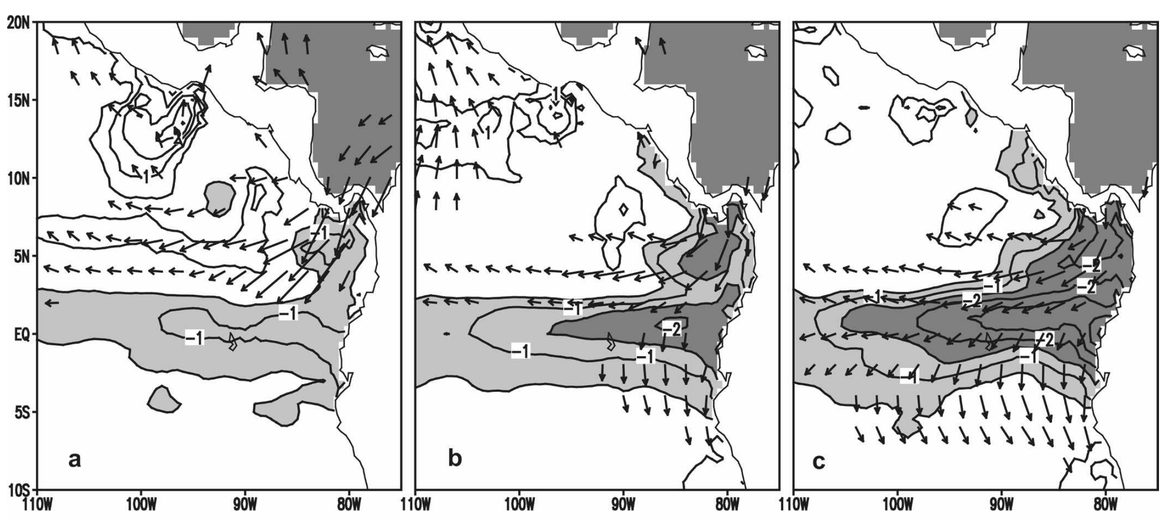

FIG. 4. Anomalies of SST (shaded <−0.5°C; zero contours omitted) and surface wind velocity (m s^{-1}) in the Atlantic cooling run of iROAM in (a) December, (b) January, and (c) February.

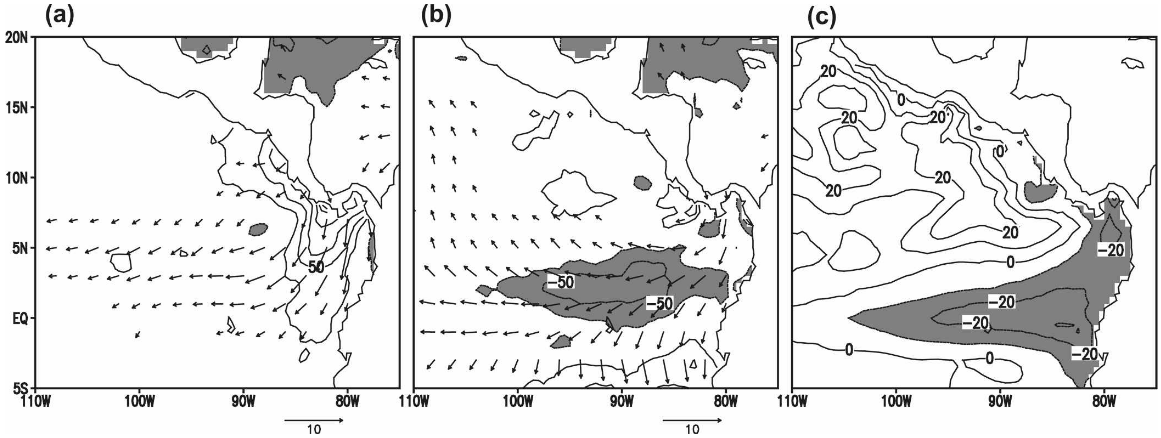

FIG. 5. March anomalies of surface wind velocity (m s^{-1}) and heat flux (positive upward at contour intervals of 25 W m^{-2} with the zero contour omitted; shaded <-25 W m^{-2}) in (a) RAM and (b) ROAM. (c) Anomalies of 20°C isotherm depth (shaded <-10 m) in ROAM.

lous Panama jet intensifies the surface turbulent (latent and sensible) heat flux from the ocean by as much as 100 W m^{-2}, by increased wind speed and by advecting anomalously cool and dry air from the Atlantic. (In the Atlantic, the decreased SST lowers the surface specific humidity by 2 g kg^{-1}.) The cold and dry advection is important for flux changes near the coast, but the wind-induced changes in turbulent heat flux dominate away from the coast.

The surface flux anomalies look very differently in the coupled model (Fig. 5b). While the Gulf of Panama loses 50–100 W m^{-2} of heat in the atmospheric model, it gains about 25 W m^{-2} in the coupled model. If the surface heat flux were the only forcing for SST, its anomalies would vanish with the SST decrease to offset the atmospheric-induced heat loss under a steady-state assumption. (The *e*-folding time scale for the mixed layer temperature adjustment is a few months.) The sign change in the heat flux anomalies over much of the Gulf of Panama indicates that subsurface ocean processes, such as increased upwelling and entrainment, are partially responsible for the SST cooling in addition to atmospheric heat flux forcing. Indeed, the thermocline shoals by 20 m in the Gulf of Panama (Fig. 5c), which along with the increased wind speed, increases the entrainment across the mixed layer bottom. The thermocline shoaling there is forced by the positive wind curls east of the axis of the anomalous Panama jet.

Figure 6 shows the coupled response to the atmospheric forcing, as represented by the difference in anomalies between the coupled and stand-alone SST-forced atmospheric modeling experiments. The cooling over the Gulf of Panama and the equatorial Pacific increases the atmospheric pressure, reducing the cross–Central American pressure difference and decelerating the anomalous Panama jet. Indeed, the Panama jet is stronger in the atmospheric than the coupled model (Figs. 5a and 5b). There is an anomalously strong Papagayo jet in the atmospheric model, which disappears in the coupled model response. Thus, the SST cooling in the Pacific is a negative feedback for the cross–Central American winds and the anomalous Panama jet in particular.

Along the equator, surface heat flux anomalies are weakly upward in the RAM run but turn downward because of the strong SST cooling that results from the Bjerknes feedback (Fig. 5). Our diagnosis of the coupled response in Fig. 6 confirms that the anomalous easterlies on the equator are coupled with the SST cooling. The ocean cooling increases the atmospheric pressure along the equator, driving divergent winds on either side of the equator. South of the equator, the equatorial cooling induces northwesterly wind anomalies, which when superimposed onto the atmospheric forcing (Fig. 5a), give rise to the C-shaped pattern of cross-equatorial wind anomalies (Fig. 4c).

b. Boreal summer/fall

The anomalies of the SST and wind on the equator decay rapidly from May onward (Fig. 3). During July–September (the climatological cold season for the equatorial Pacific), weak SST anomalies of -1°C linger in a narrow band north of the equator, representing a sharpening of the SST front there (Fig. 7c). Climatologically, this SST front develops north of the equator during the cold season, separating the cold tongue to the south and the warm band to the north. De Szoeke et al. (2007) study the formation mechanisms for this equatorial front in the iROAM. The cooling that lingers on the equatorial front and off of Panama is main-

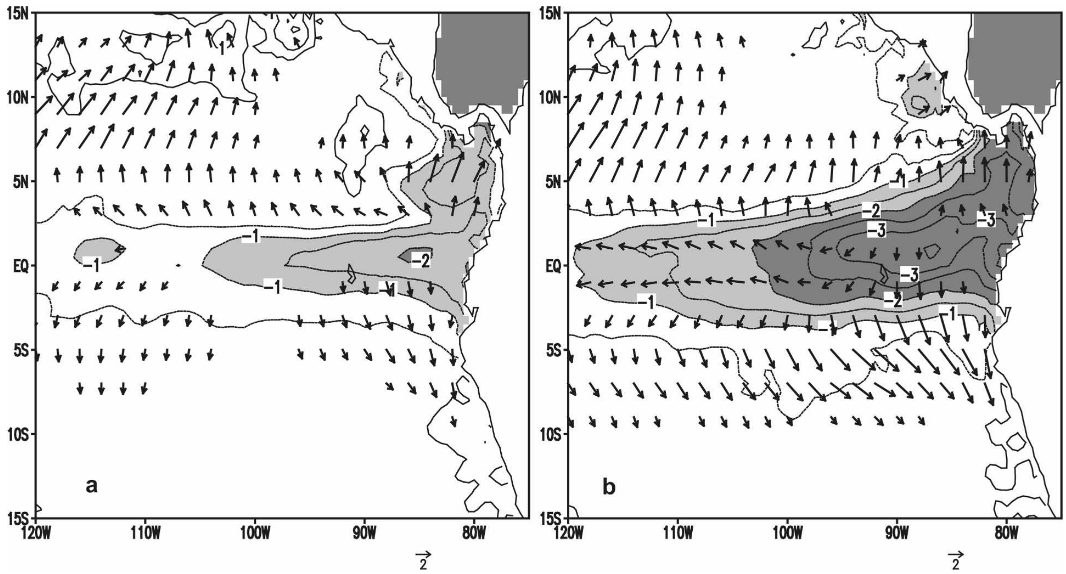

FIG. 6. Coupled response of the Pacific to Atlantic cooling in (a) January and (b) March: (NAC − CTRL) minus (NACa − CTRLa) differences in SST (shaded <-1°C; zero contours omitted) and surface wind velocity (m s^{-1}).

tained by subsurface ocean processes as the surface heat flux acts as a damping there (Fig. 7b).

Near the Central American coast, the northeasterly wind anomalies persist across Panama but do not penetrate far southward (Figs. 7a and 7b). Wind anomalies cover a much broader area during summer/fall than winter/spring, blowing across the entire Central American isthmus. Somewhat counterintuitively, SST increases in a broad region west of Central America despite the strong SST cooling imposed on the other side of the isthmus. The warming occurs because the broad easterly wind anomalies weaken the climatological southwesterlies (cf. Fig. 2b) and reduce evaporative cooling from the ocean. In RAM, the downward heat flux anomalies amounts to 80 W m^{-2} (Fig. 7a), with the wind-induced decrease in evaporation and solar radiation increase contributing about equally. This heat flux forcing is nearly compensated by the SST warming effect in ROAM (Fig. 7b). The broad SST warming centered along 10°N exerts a discernible feedback to the atmosphere, slightly increasing the local precipitation compared to RAM and inducing a moderate cyclonic circulation at the surface (Fig. 7c).

Overall, the atmospheric response is much larger

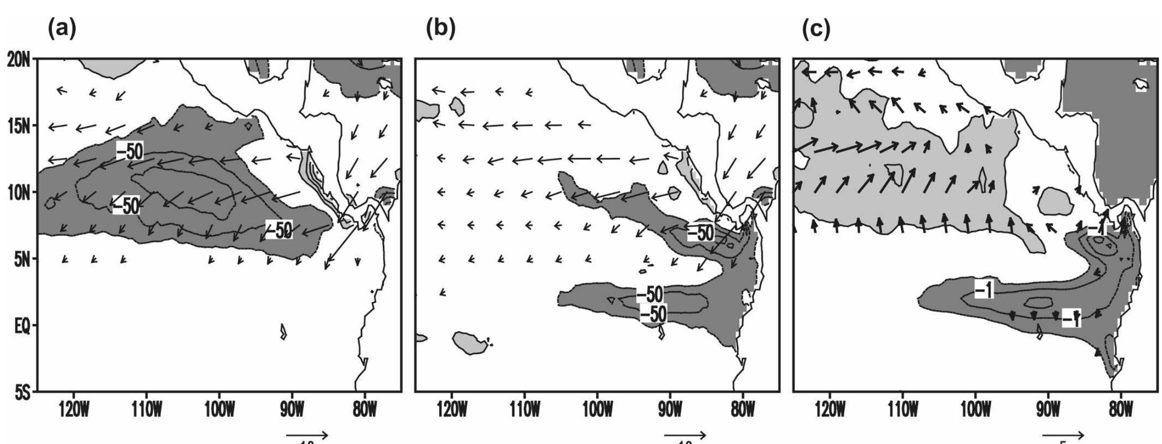

FIG. 7. July–September anomalies of surface wind velocity (m s^{-1}) and heat flux (positive upward with the zero contour omitted; dark shading <-25; light shading >25 W m^{-2}) in (a) RAM and (b) ROAM. (c) July–September coupled response to the Atlantic cooling: (NAC − CTRL) minus (NACa − CTRLa) differences in SST (dark shading <-0.5°C; light shading >0.5°C) and surface wind velocity (m s^{-1}).

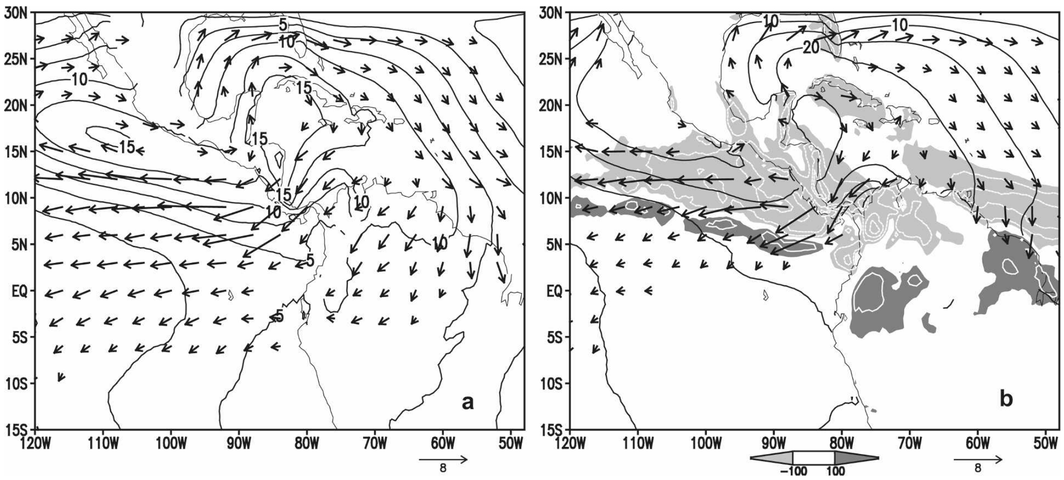

FIG. 8. July iROAM anomalies of wind velocity (m s^{-1}), and geopotential height at (a) 850 and (b) 1000 hPa. Contour intervals are 2.5 and 5 m in (a) and (b), respectively. In (b) precipitation anomalies are shown in gray shade and in white contours at internals of 100 mm month^{-1}.

during summer than winter/spring because the tropical North Atlantic is climatologically warmer and hence conducive to atmospheric convection. In addition, the Pacific ITCZ, moving northward to latitudes just west of the Central American isthmus, is more susceptible to Atlantic influences. As a measure of this seasonal difference, the maximum anomalies of the sea level pressure on the Atlantic coast of the isthmus are 4 and 2 hPa during boreal summer and winter, respectively. Sutton and Hodson (2007) note a similar tendency for atmospheric circulation anomalies to grow during boreal summer/fall in response to North Atlantic SST anomalies in their atmospheric GCM. In the Atlantic sector, the imposed cooling reduces precipitation in the Gulf of Mexico, the Caribbean, and the ITCZ (Fig. 8b). There is also a tendency for the southward displacement of the ITCZ, with some slight increase in rainfall over equatorial South America.

The general decrease in rainfall over the tropical Atlantic increases the atmospheric pressure and forces an anticyclonic circulation. (Over the tropical Atlantic, the westward increase of the pressure anomalies is characteristic of the Rossby wave response to the SST cooling, as by construction, the anomalies are set to zero at lateral boundaries in the regional model.) The anomalous anticyclonic system has a deep baroclinic structure and propagates westward through the Central American isthmus (~1 km high in elevation). Figure 9 shows the vertical structure of the subsidence Rossby wave along 12°N, which together with the orographic subsidence induced by the anomalous surface northeasterlies across the isthmus, reduces the humidity and suppresses convection in the Pacific ITCZ.

The decreased precipitation on both sides of the isthmus is consistent with paleo-observations during Heinrich events and the Younger Dryas (Schmidt et al. 2006; Kienast et al. 2006; Leduc et al. 2007). It is interesting to note that there is a narrow ribbon of increased precipitation over the eastern Pacific just south of the broader decrease in rainfall. This rainfall increase is associated with low-level wind convergence. A sediment core analysis by Pahnke et al. (2007) shows an increasing tendency in precipitation there during the Heinrich 1 event 15 kyr BP. The broad easterly wind anomalies are in geostrophic balance with the anomalous high to the

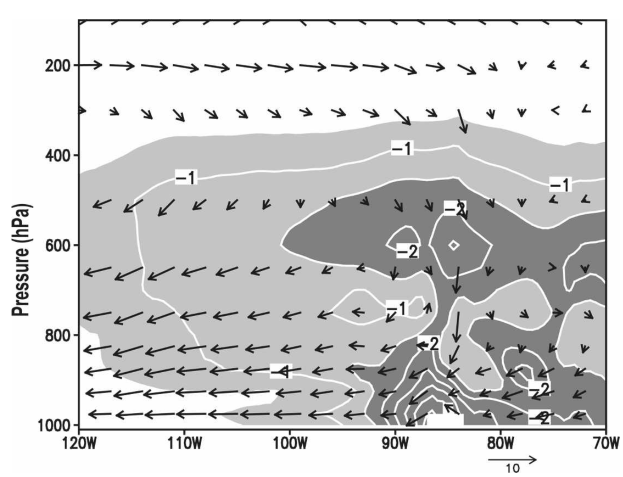

FIG. 9. July RAM anomalies of zonal (m s^{-1}) and vertical ($-\omega$, Pa s^{-1}) velocities (vectors), and specific humidity (shaded and contours, g kg^{-1}) at 12°N in the iRAM. The vector scale at the lower right is for the zonal velocity while the pressure velocity is scaled up by a factor of 25 for clarity.

north, weakening the prevailing southwesterlies and causing a weak warming in SST. Thus, the weak warming under the Pacific ITCZ is likely a result of the anticyclonic Rossby wave instead of the cause of the weakened ITCZ.

c. Stability effect

Given that the atmospheric response to the Atlantic cooling is much stronger in boreal summer than winter, the question arises as to why the equatorial Pacific SST response is much weaker in summer? During boreal summer, the deepening of the thermocline along the 5°N trough (Fig. 2) hampers the propagation of the SST cooling off of Panama onto the equator, and the prevailing climatological southwesterlies in the CTRL prevent the advection of the cold and dry air from the Atlantic. The northeast wind anomalies superimposed on the mean southwesterlies can even cause a weak warming in the northeastern Pacific.

Figure 8 reveals another reason for selecting boreal winter as the season for a stronger equatorial Pacific response. While the easterly wind anomalies during boreal summer extend from the ITCZ southward across the equator at 850 hPa, they decay rapidly south of 10°N and virtually vanish on the equator at the sea surface. Figure 10 shows the seasonal evolution of the vertical structure of the zonal wind velocity at the equator. While the easterly anomalies at 800 hPa do not change very much at about -3 m s^{-1} throughout the year, strong vertical shears develop from May to November, coinciding with the climatological development of the cold tongue. The seasonal cooling of the equatorial Pacific strengthens the stratification of the atmospheric boundary layer and decouples the surface wind from the free troposphere. The potential temperature difference between 800 hPa and the surface increases from 6 to 10 K in the CTRL from March to September. An alternative explanation is that the SST cooling decreases the atmospheric boundary layer depth and the resultant increase in the depth-averaged friction slows down the boundary layer wind driven by the pressure perturbation in the free troposphere (Samelson et al. 2006).

Such an increase in atmospheric stratification over the cold tongue, often in the form of an internal atmospheric inversion, is observed in atmospheric soundings over the eastern Pacific, associated with a sharp reduction in surface wind velocity (Hashizume et al. 2002; Raymond et al. 2004). The effects of the SST modulation of the vertical wind shear are commonly observed by satellite, as is manifested in the high correlation between the SST and surface wind anomalies (Liu et al. 2000; Chelton et al. 2001; Hashizume et al. 2001). See Xie (2004) and Small et al. (2008) for recent reviews on the topic of SST–surface wind coupling.

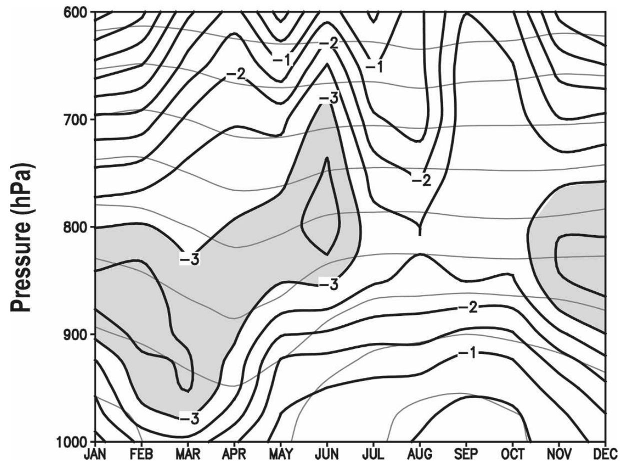

FIG. 10. Time–pressure cross section of the zonal wind anomalies (black contours; shaded <-3 m s^{-1}) and climatological potential temperature (thin gray contours at intervals of 2.5 K) in iROAM, averaged in 2°S–2°N, 110°–90°W.

The atmospheric teleconnection from the Atlantic reaches the Pacific across the mountains of Central America as Rossby waves in the free troposphere. While the easterly wind anomalies remain strong in the free troposphere year round, they are very weak at the surface as the seasonal development of the cold tongue reduces the vertical momentum mixing. We note, however, that the strong easterly wind anomalies in the atmospheric boundary layer during January–April are not only due to enhanced vertical mixing that brings wind anomalies to the surface, but also driven by anomalous SST gradients along the equator. As the surface zonal wind anomalies on the equator are an important trigger for the Bjerknes feedback, the SST modulation of the vertical wind shear and surface wind is an important factor leading to the seasonality of the equatorial Pacific response.

4. Summary and discussion

We have investigated the Pacific response to an SST cooling over the tropical North Atlantic using a regional coupled model. The Atlantic cooling increases the atmospheric pressure over the Caribbean Sea, driving anomalous northeasterly winds across Central America. Strong SST cooling takes place under these northeasterly anomalies in the Gulf of Panama, especially during boreal winter/spring when the climatological mean northeast trades prevail in the mean and blow across the Central American isthmus. This Gulf of Panama cooling reaches the equator during boreal winter where an anomalously strong cold tongue develops that is amplified by the Bjerknes-type interaction of SST, zonal wind, and the thermocline depth. This equatorial cooling, attaining values of up to 3°C in magnitude, is most pronounced during March–April and represents a considerable weakening of the SST annual cycle on the equator.

The atmospheric response to the Atlantic cooling, as measured by the atmospheric pressure increase and anomalous cross-isthmus winds, is much stronger during boreal summer than winter because the North Atlantic is warmer and conducive to deep convection in summer. Despite this strong atmospheric response in summer, the equatorial Pacific response favors the winter/spring and decays rapidly in early summer. Our results suggest that the following factors favor a strong equatorial Pacific response in boreal spring.

1) Mean northeast trades across Central America during winter/spring. The mean cross-isthmus winds advect the anomalously cool and dry air from the North Atlantic and help cool the Pacific off of Central America with enhanced surface turbulent heat flux and entrainment at the bottom of the ocean mixed layer. The northeasterly wind anomalies, maintained year round by the Atlantic cooling, preferentially cool the Pacific via surface flux during the seasons with the prevailing winds in the same direction.
2) A shoaling thermocline along the 5°N trough. The positive wind curls of the southward migration of the ITCZ lift the thermocline in a zonal belt between the Central American coast and the equator, facilitating the equatorward propagation of the SST cooling originating from the Gulf of Panama. The shoaling thermocline amplifies the SST response to wind not only by reducing the heat content of the mixed layer but also by increasing the effects of upwelling and entrainment.
3) SST modulation of surface winds on the equator. The North Atlantic cooling forces subsidence Rossby waves that propagate into the Pacific through Central America. The anomalous easterlies associated with these Rossby waves, while decaying southward, persist year round in the lower free troposphere over the equatorial Pacific. The development of the climatological cold tongue during summer/fall increases the stratification of the atmospheric boundary layer, preventing the easterly wind anomalies in the free troposphere from reaching the surface. The deceleration of surface easterly anomalies in response to the seasonal development of the mean cold tongue contributes to the rapid decay of anomalous SST cooling on the equator.

a. Comparison with GCM hosing experiments

In response to the AMOC shutdown, the development of anomalous northeasterly wind anomalies across Central America is a feature common among all the GCMs (Timmermann et al. 2007; see model details therein). Figure 11 compares wind and SST anomalies among GCMs and with the iROAM NAC run. As summarized above, our study suggests that the atmospheric forcing of Pacific SST anomalies and their amplification due to the Bjerknes feedback is strongest during boreal winter/spring. This finding is consistent with the simulated wind and SST response during January–May in the CGCM water-hosing experiments. The SST cooling on and north of the equator is most pronounced during this period. South of the equator, the anomalous southwesterlies induce weak warming. The results begin to diverge among models from May–June onward. Thereafter, the GFDL Coupled Community Model, version 2.1 (CM2.1), and the Third Hadley Centre Coupled Ocean–Atmosphere GCM (HadCM3) develop a pronounced SST dipole with the C-shaped wind pattern characteristic of the WES feedback. SST anomalies decay in ECHAM5-OM1 and in the Community Climate System Models, versions 2 and 3 (CCSM2 and CCSM3), while the northeasterly wind anomalies remain strong off of Central America, much as in iROAM. Unlike iROAM, however, summer/fall SST anomalies do not turn positive in GCMs under the northeasterly anomalies. This difference can be explained in terms of the differences in the simulated climatological winds. During summer, the climatological winds are southwesterly south of the Pacific ITCZ toward Central America both in the observations (Fig. 1b) and iROAM (Fig. 2b). However, the climatological summer westerly wind component is too weak or even easterly in coupled GCMs (not shown). The climatological wind field determines the sign of the SST response to the anomalous easterlies in water-hosing runs.

Thus, the strong atmospheric forcing on the SST during winter/spring appears to be responsible for the consistent Pacific SST response in GCM water-hosing runs. The Pacific anomalies begin to differ among models from early summer possibly because the Atlantic influence becomes less effective on the SST, allowing models to develop their own favorite modes. It is still unclear why some models choose to develop a WES-type response after spring. It is well known that the Pacific climatology simulated in nearly all the GCMs is too symmetrical about the equator (de Szoeke and Xie 2008), and a symmetrical climatology favors the development of the meridional dipole mode by the WES

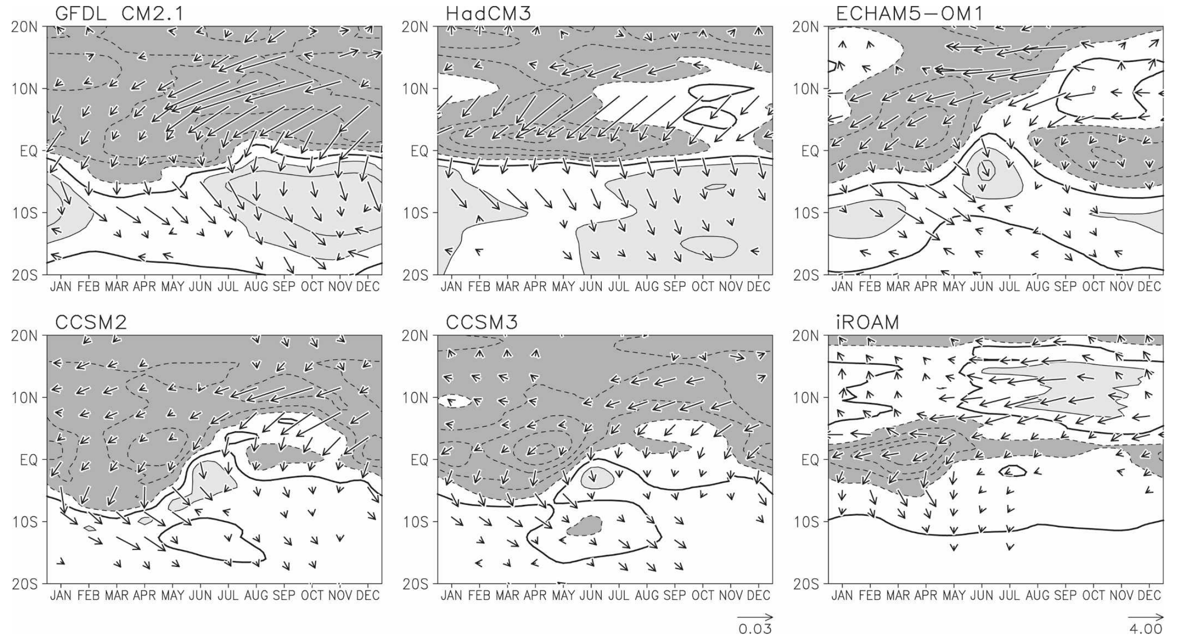

FIG. 11. Time–latitude cross sections of SST (contour intervals of 0.5°C; dark shading <−0.5 and light shading >0.5°C) and anomalous surface wind vectors averaged in 120°–80°W in response to the AMOC shutdown in five GCMs and to Atlantic cooling in iROAM. Vectors are for wind stress (N m^{-2}) for GCMs and wind velocity (m s^{-1}) for iROAM.

feedback (Okajima et al. 2003). Curiously, the HadCM3 develops the meridional dipole mode while CCSM2 and -3 do not, despite that the former develops a stronger meridional asymmetry in the Pacific climatology (de Szoeke and Xie 2008). Obviously, much needs to be learned about the Pacific response during the summer/fall seasons.

High-resolution paleoclimate reconstructions off the Pacific coast of Central America, and especially in the Gulf of Panama (Kienast et al. 2006; Leduc et al. 2007; Pahnke et al. 2007), provide an important test bed for the ideas discussed here and might help to identify the meridional structure of the Pacific response to an AMOC shutdown in more detail. While high compared to GCMs, the resolution of the iROAM is still insufficient for a truly adequate representation of the Isthmus of Panama and the narrow mountains. For example, the Panama wind jet during winter/spring does not extend far enough south and veers away from the South American coast (Fig. 2a versus Fig. 1a). The latter error is important for coastal upwelling. Figure 12 shows the February–August difference in sea surface height (SSH) based on the merged satellite altimeter product of Ducet et al. (2000). The observed Panama jet hugs the South American coast, raising the thermocline offshore by both coastal and open-ocean upwelling (Rodriquez-Rubio et al. 2003; Xie et al. 2005). The February–August SSH difference there amounts to 20 cm (Fig. 12), equivalent to a thermocline shoaling of 60 m for a typical reduced gravity of 0.3 m s^{-2}. Farther to the west, around 90°–85°W, the SSH difference is small and even slightly positive from February to August because of complicated wind curl structures forced by Central American mountains. Thus, in reality, we expect that large SST cooling during Heinrich events and Younger Dryas is even more confined in space than in iROAM, along the meridional band near the coast with a strong thermocline shoaling during boreal winter (Fig. 12).

The cross–Central American moisture transport is a major reason why the North Atlantic is favored for the

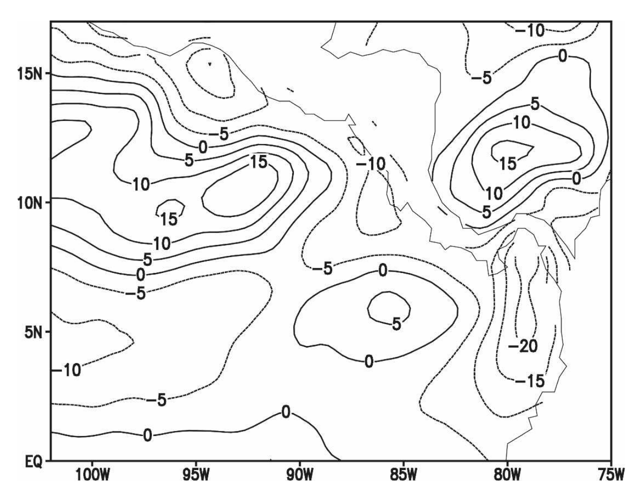

FIG. 12. February–August difference in observed sea surface height (cm) climatology.

sinking branch of the global meridional overturning circulation (e.g., Broecker 1997). How the AMOC shutdown affects this cross-ocean moisture transport is under debate in the recent literature. Some argue that the North Atlantic cooling depresses atmospheric humidity and reduces the moisture transport (Leduc et al. 2007) while some point to the accelerated northeasterlies across Central America as a mechanism for intensified transport (Pahnke et al. 2007). In iROAM, the effect of increased mass transport is larger than the effect of atmospheric drying, and the net moisture transport across Central America increases in response to the North Atlantic cooling (I. Richter 2007, personal communication). Thus, the moisture transport appears to be a negative feedback that increases North Atlantic salinity and acts to restore the AMOC after it is shut down by freshwater forcing.

b. Implications for the present climate

In instrumental observations, ENSO dominates tropical climate variability. It is well known that El Niño induces atmospheric teleconnections that relax the northeast trades and causes a delayed SST warming over the Caribbean Sea and northwestern tropical Atlantic (Enfield and Mayer 1997). There are other modes of tropical North Atlantic anomalies such as the tropical meridional mode (Chang et al. 1997; Xie and Tanimoto 1998) and the size change in the Atlantic warm pool (Wang et al. 2006). In addition, the Atlantic multidedacal oscillation (AMO; Enfield et al. 2001) is emerging as a mode of ocean–atmospheric variability possibly involving the AMOC (Delworth and Mann 2000; Knight et al. 2005), with widespread influences on the atmospheric circulation, precipitation, and possibly even Atlantic hurricanes (Goldenberg et al. 2001; Sutton and Hodson 2005, 2007; Zhang and Delworth 2006). Results from GCM water-hosing experiments and our NAC run can elucidate how tropical North Atlantic SST anomalies influence the Pacific. There is some evidence that the cold phase of the observed AMO reduces the annual cycle over the equatorial Pacific (Timmermann et al. 2007), a result consistent with the model response in the Pacific. The changes in the annual cycle could affect the amplitude and phasing of ENSO (Timmermann et al. 2007).

In iROAM, the North Atlantic cooling suppresses atmospheric convection both locally and remotely over Central America and the far eastern tropical Pacific. Similar simultaneous decreases in rainfall over the Gulf of Mexico, the Caribbean, Central America, and the far eastern Pacific warm pool have a counterpart in the current climate known as the midsummer drought (MSD). Over these regions, precipitation begins to increase from May to June but decreases rather mysteriously during July–August, and then recovers in September (Magana et al. 1999; Small et al. 2007). Mapes et al. (2005) suggest that the westward development of the basin-scale subtropical high over the North Atlantic from June to July is instrumental in the MSD onset. Our NAC run supports this hypothesis with an explicit demonstration. In fact, the imposed forcing is limited to the Atlantic Ocean but the atmospheric response propagates its effects into the Pacific through Central America in the form of the subsidence Rossby wave. The suppressed convection in the Pacific ITCZ reinforces the anticyclonic Rossby wave, which propagates farther westward. We note broadly similar results from an independent study of the response of an atmospheric GCM to prescribed changes in the Atlantic warm pool (Wang et al. 2008). Over the Pacific, SST anomalies are a secondary effect for the suppression of convection in iROAM, in support of Small et al.'s (2007) hypothesis based on observations. In our NAC run, summer Pacific SST increases slightly in response to the weakened westerlies and increased solar radiation. The SST increase acts to enhance, instead of suppress, local convection over the eastern Pacific warm pool.

Acknowledgments. We wish to thank the iROAM team at IPRC and FRCGC for developing the model. The iROAM experiments were performed on the Earth Simulator. This work is supported by NOAA, NASA, JAMSTEC, and the Kyosei-7 Project.

REFERENCES

Broecker, W. S., 1997: The thermohaline circulation, the Achilles heel of our climate system: Will man-made CO_2 upset the current balance? *Science,* **278,** 1582–1588.

Chang, P., L. Ji, and H. Li, 1997: A decadal climate variation in the tropical Atlantic Ocean from thermodynamic air–sea interactions. *Nature,* **385,** 516–518.

——, and Coauthors, 2006: Climate fluctuations of tropical coupled system—The role of ocean dynamics. *J. Climate,* **19,** 5122–5174.

Chelton, D. B., M. H. Freilich, and S. N. Esbensen, 2000: Satellite observations of the wind jets off the Pacific coast of Central America. Part I: Case studies and statistical characteristics. *Mon. Wea. Rev.,* **128,** 1993–2018.

——, and Coauthors, 2001: Observations of coupling between surface wind stress and sea surface temperature in the eastern tropical Pacific. *J. Climate,* **14,** 1479–1498.

Chiang, J. C. H., 2004: Present-day climate variability in the tropical Atlantic: A model for paleoclimate changes? *The Hadley Circulation: Past, Present, and Future,* H. F. Diaz and R. Bradley, Eds, Springer, 465–488.

——, M. Biasutti, and D. S. Battisti, 2003: Sensitivity of the Atlantic ITCZ to conditions during Last Glacial Maximum boundary conditions. *Paleoceanography,* **18,** 1094, doi:10.1029/2003PA000916.

——, W. Cheng, and C. M. Bitz, 2008: Fast teleconnections to the tropical Atlantic sector from Atlantic thermohaline adjustment. *Geophys. Res. Lett.,* **35,** L07704, doi:10.1029/2008GL033292.

Dahl, K. A., A. J. Broccoli, and R. J. Stouffer, 2005: Assessing the role of North Atlantic freshwater forcing in millennial scale climate variability: A tropical Atlantic perspective. *Climate Dyn.,* **24,** 325–346.

Delworth, T. L., and M. E. Mann, 2000: Observed and simulated multidecadal variability in the Northern Hemisphere. *Climate Dyn.,* **16,** 661–676.

de Szoeke, S. P., and S.-P. Xie, 2008: The tropical eastern Pacific seasonal cycle: Assessment of errors and mechanisms in IPCC AR4 coupled ocean–atmosphere general circulation models. *J. Climate,* **21,** 2573–2590.

——, Y. Wang, S.-P. Xie, and T. Miyama, 2006: The effect of shallow cumulus convection on the eastern Pacific climate in a coupled model. *Geophys. Res. Lett.,* **33,** L17713, doi:10.1029/2006GL026715.

——, S.-P. Xie, T. Miyama, K. J. Richards, and R. J. O. Small, 2007: What maintains the SST front north of the equatorial cold tongue? *J. Climate,* **20,** 2500–2514.

Dong, B.-W., and R. T. Sutton, 2002: Adjustment of the coupled ocean–atmosphere system to a sudden change in the thermohaline circulation. *Geophys. Res. Lett.,* **29,** 1728, doi:10.1029/2002GL015229.

Ducet, N., P. Y. Le Traon, and G. Reverdin, 2000: Global high-resolution mapping of ocean circulation from TOPEX/Poseidon and ERS-1 and -2. *J. Geophys. Res.,* **105,** 19 477–19 498.

Enfield, D. B., and D. A. Mayer, 1997: Tropical Atlantic SST variability and its relation to El Nino–Southern Oscillation. *J. Geophys. Res.,* **102,** 929–945.

——, A. M. Mestas-Nuñez, and P. J. Trimble, 2001: The Atlantic multidecadal oscillation and its relation to rainfall and river flows in the continental U.S. *Geophys. Res. Lett.,* **28,** 2077–2080.

Goldenberg, S. B., C. W. Landsea, A. M. Mestas-Nuñez, and W. M. Gray, 2001: The recent increase in Atlantic hurricane activity: Causes and implications. *Science,* **293,** 474–479.

Hashizume, H., S.-P. Xie, W. T. Liu, and K. Takeuchi, 2001: Local and remote atmospheric response to tropical instability waves: A global view from the space. *J. Geophys. Res.,* **106,** 10 173–10 185.

——, ——, M. Fujiwara, M. Shiotani, T. Watanabe, Y. Tanimoto, W. T. Liu, and K. Takeuchi, 2002: Direct observations of atmospheric boundary layer response to SST variations associated with tropical instability waves over the eastern equatorial Pacific. *J. Climate,* **15,** 3379–3393.

Haug, G. H., K. A. Hughen, D. M. Sigman, L. C. Peterson, and U. Rohl, 2001: Southward migration of the intertropical convergence zone through the Holocene. *Science,* **293,** 1304–1308.

Hemming, S. R., 2004: Heinrich events: Massive late Pleistocene detritus layers of the North Atlantic and their global climate imprint. *Rev. Geophys.,* **42,** RG1005, doi:10.1029/2003RG000128.

Hu, A., B. L. Otto-Bliesner, G. A. Meehl, W. Han, C. Morrill, E. C. Brady, and B. Briegleb, 2008: Response of thermohaline circulation to freshwater forcing under present-day and LGM conditions. *J. Climate,* **21,** 2239–2258.

Kalnay, E., and Coauthors, 1996: The NCEP/NCAR 40-Year Reanalysis Project. *Bull. Amer. Meteor. Soc.,* **77,** 437–471.

Kessler, W. S., 2006: The circulation of the eastern tropical Pacific: A review. *Prog. Oceanogr.,* **69,** 181–217.

Kienast, M., S. S. Kienast, S. E. Calvert, T. I. Eglinton, G. Mollenhauer, R. Francois, and A. C. Mix, 2006: Eastern Pacific cooling and Atlantic overturning circulation during the last deglaciation. *Nature,* **443,** 846–849.

Knight, J. R., R. J. Allan, C. K. Folland, M. Vellinga, and M. E. Mann, 2005: A signature of persistent natural thermohaline circulation cycles in observed climate. *Geophys. Res. Lett.,* **32,** L20708, doi:10.1029/2005GL024233.

Krebs, U., and A. Timmermann, 2007: Tropical air–sea interactions accelerate the recovery of the Atlantic Meridional Overturning Circulation after a major shutdown. *J. Climate,* **20,** 4940–4956.

Leduc, G., L. Vidal, K. Tachikawa, F. Rostek, C. Sonzogni, L. Beaufort, and E. Bard, 2007: Moisture transport across Central America as a positive feedback on abrupt climatic changes. *Nature,* **445,** 908–911.

Levitus, S., 1982: *Climatological Atlas of the World Ocean*. NOAA Prof. Paper No. 13, 173 pp. and 17 microfiche.

Liu, W. T., X. Xie, P. S. Polito, S.-P. Xie, and H. Hashizume, 2000: Atmospheric manifestation of tropical instability waves observed by QuikSCAT and Tropical Rain Measuring Mission. *Geophys. Res. Lett.,* **27,** 2545–2548.

Magana, V., J. A. Amador, and S. Medina, 1999: The midsummer drought over Mexico and Central America. *J. Climate,* **12,** 1577–1588.

Manabe, S., and R. J. Stouffer, 1995: Simulation of abrupt climate change induced by freshwater input to the North Atlantic Ocean. *Nature,* **378,** 165–167.

Mapes, B. E., P. Liu, and N. Buenning, 2005: Indian monsoon onset and the Americas midsummer drought: Out-of-equilibrium responses to smooth seasonal forcing. *J. Climate,* **18,** 1109–1115.

Menviel, L., A. Timmermann, A. Mouchet, and O. Timm, 2008: Meridional reorganizations of marine and terrestrial productivity during glacial Heinrich events. *Paleoceanography*, PA1203, doi:10.1029/2007PA001445.

Mitchell, T. P., and J. M. Wallace, 1992: The annual cycle in equatorial convection and sea surface temperature. *J. Climate,* **5,** 1140–1156.

Pacanowski, R. C., 1996: Documentation user's guide and reference manual of MOM2, Version 2. GFDL Ocean Tech. Rep. 3.2, Princeton, NJ, 329 pp.

Pahnke, K., J. Sachs, L. Keigwin, A. Timmermann, and S.-P. Xie, 2007: Eastern tropical Pacific hydrologic changes during the past 27, 000 years from D/H ratio in alkenones. *Paleoceanography*, PA4214, doi:10.1029/2007PA001468.

Peterson, L. C., G. H. Haug, K. A. Hughen, and U. Rohl, 2000: Rapid changes in the hydrologic cycle of the tropical Atlantic during the last glacial. *Science,* **290,** 1947–1951.

Okajima, H., S.-P. Xie, and A. Numaguti, 2003: Interhemispheric coherence of tropical climate variability: Effect of climatological ITCZ. *J. Meteor. Soc. Japan,* **81,** 1371–1386.

Raymond, D. J., and Coauthors, 2004: EPIC2001 and the coupled ocean–atmosphere system of the tropical east Pacific. *Bull. Amer. Meteor. Soc.,* **85,** 1341–1354.

Rodriquez-Rubio, E., W. Schneider, and R. A. del Rio, 2003: On the seasonal circulation within the Panama Bight derived from satellite observations of wind, altimetry, and sea surface temperature. *Geophys. Res. Lett.,* **30,** 1410, doi:10.1029/2002GL016794.

Samelson, R. M., E. D. Skyllingstad, D. B. Chelton, S. K. Esbensen, L. W. O'Neill, and N. Thum, 2006: On the coupling of wind stress and sea surface temperature. *J. Climate,* **19,** 1557–1566.

Schmidt, M. W., M. J. Vautravers, and H. J. Spero, 2006: Rapid subtropical North Atlantic salinity oscillations across Dansgaard-Oeschger cycles. *Nature,* **443,** 561–564.

Small, R. J. O., S. P. de Szoeke, and S.-P. Xie, 2007: The Central American midsummer drought: Regional aspects and large-scale forcing. *J. Climate,* **20,** 4853–4873.

——, and Coauthors, 2008: Air–sea interaction over ocean fronts and eddies. *Dyn. Atmos. Ocean,* in press.

Stott, L., C. Poulsen, S. Lund, and R. Thunell, 2002: Super ENSO and global climate oscillations at millennial time scales. *Science,* **297,** 222–226.

Stouffer, R., and Coauthors, 2006: Investigating the causes of the response of the thermohaline circulation to past and future climate changes. *J. Climate,* **19,** 1365–1387.

Sutton, R. T., and D. L. Hodson, 2005: Atlantic Ocean forcing of North American and European summer climate. *Science,* **309,** 115–118.

——, and ——, 2007: Climate response to basin-scale warming and cooling of the North Atlantic Ocean. *J. Climate,* **20,** 891–907.

Tanimoto, Y., and S.-P. Xie, 2002: Inter-hemispheric decadal variations in SST, surface wind, heat flux and cloud cover over the Atlantic Ocean. *J. Meteor. Soc. Japan,* **80,** 1199–1219.

Timmermann, A., M. Latif, R. Voss, and A. Groetzner, 1998: Northern Hemispheric interdecadal variability: A coupled air–sea mode. *J. Climate,* **11,** 1906–1931.

——, and Coauthors, 2007: The influence of a weakening of the Atlantic meridional overturning circulation on ENSO. *J. Climate,* **20,** 4899–4919.

Vellinga, M., and R. Wood, 2002: Global climate impacts of a collapse of the Atlantic thermohaline circulation. *Climatic Change,* **54,** 251–267.

Wang, C., D. B. Enfield, S. K. Lee, and C. W. Landsea, 2006: Influences of the Atlantic warm pool on Western Hemisphere summer rainfall and Atlantic hurricanes. *J. Climate,* **19,** 3011–3028.

——, S. K. Lee, and D. B. Enfield, 2008: Climate response to anomalously large and small Atlantic warm pools during the summer. *J. Climate,* **21,** 2437–2450.

Wang, Y., S.-P. Xie, H. Xu, and B. Wang, 2004: Regional model simulations of marine boundary layer clouds over the southeast Pacific off South America. Part I: Control experiment. *Mon. Wea. Rev.,* **132,** 274–296.

Wu, L., F. He, Z. Liu, and C. Li, 2007: Atmospheric teleconnection of tropical Atlantic variability: Interhemispheric, tropical–extratropical and cross-basin interaction. *J. Climate,* **20,** 856–870.

——, C. Li, C. Yang, and S.-P. Xie, 2008: Global teleconnections in response to a shutdown of the Atlantic meridional overturning circulation. *J. Climate,* **21,** 3002–3019.

Xie, S.-P., 2004: Satellite observations of cool ocean–atmosphere interaction. *Bull. Amer. Meteor. Soc.,* **85,** 195–208.

——, and S. G. H. Philander, 1994: A coupled ocean–atmosphere model of relevance to the ITCZ in the eastern Pacific. *Tellus,* **46A,** 340–350.

——, and Y. Tanimoto, 1998: A pan-Atlantic decadal climate oscillation. *Geophys. Res. Lett.,* **25,** 2185–2188.

——, and J. A. Carton, 2004: Tropical Atlantic variability: Patterns, mechanisms, and impacts. *Earth Climate: The Ocean-Atmosphere Interaction, Geophys. Monogr.,* Vol. 147, Amer. Geophys. Union, 121–142.

——, H. Xu, W. S. Kessler, and M. Nonaka, 2005: Air–sea interaction over the eastern Pacific warm pool: Gap winds, thermocline dome, and atmospheric convection. *J. Climate,* **18,** 5–25.

——, and Coauthors, 2007: A regional ocean–atmosphere model for eastern Pacific climate: Towards reducing tropical biases. *J. Climate,* **20,** 1504–1522.

Xu, H., S.-P. Xie, Y. Wang, and R. J. Small, 2005: Effects of Central American mountains on the eastern Pacific winter ITCZ and moisture transport. *J. Climate,* **18,** 3856–3873.

Zhang, R., and T. Delworth, 2005: Simulated tropical response to a substantial weakening of the Atlantic thermohaline circulation. *J. Climate,* **18,** 1853–1860.

——, and ——, 2006: Impact of Atlantic multidecadal oscillations on India/Sahel rainfall and Atlantic hurricanes. *Geophys. Res. Lett.,* **33,** L17712, doi:10.1029/2006GL026267.